Clays and Clay Minerals, Vol. 45, No. 5, 745–760, 1997.

THE EFFECT OF ADDED POLYMERS ON *n*-BUTYLAMMONIUM VERMICULITE SWELLING

M. V. SMALLEY,[1] H. JINNAI,[1] T. HASHIMOTO[1,2] AND S. KOIZUMI[3]

[1] Hashimoto Polymer Phasing Project, ERATO, JRDC, Keihanna Plaza, 1-7 Hikari-dai, Seika-cho, Kyoto 619-02, Japan

[2] Department of Polymer Chemistry, Graduate School of Engineering, Kyoto University, Kyoto 606, Japan

[3] Neutron Scattering Laboratory, Department of Materials Science and Engineering, Japan Atomic Energy Research Institute, Tokai-mura 319-11, Japan

Abstract—A 4-component clay–polymer–salt–water system was studied by neutron scattering. The clay–salt–water system consisted of *n*-butylammonium vermiculite, *n*-butylammonium chloride and heavy water, and the volume fraction of clay in the system was held constant, at $r = 0.01$. Three polymers in the molecular weight range 10,000 to 30,000 were studied, poly(vinyl methyl ether) (PVME), poly(ethylene oxide) (PEO) and poly(acrylic acid) (PAA), at a polymer volume fraction of $v = 0.01$. The addition of PAA suppressed the clay swelling, irrespective of the salt concentration, c. The addition of the neutral polymers had no effect on the phase transition temperature, T_c, between the gel and tactoid phases of the system, its value remaining at 14 °C for $c = 0.1$ *M* and 30 °C for $c = 0.01$ *M*. At $c = 0.01$ *M*, the neutral polymers also had a negligible effect on the lattice constant d along the swelling axis of the clay colloid, but at $c = 0.1$ *M*, the d-value was significantly lower than in the system without added polymer. For a PVME sample of molecular weight 18,000, both d and T_c were measured as a function of v, for volume fractions between 0 and 0.04. The addition of polymer, up to $v = 0.04$, had no effect on T_c. However, even for v values as low as 0.001, the vermiculite layers in the gel phase were more parallel and more regularly spaced than in the system without added polymer. In the gel phase, d decreased exponentially as a function of v, from 12 nm at $v = 0$ to 8 nm at $v = 0.04$. In the tactoid phase, at $T > 14$ °C, the d-value in the crystalline regions was equal to 1.94 nm at $v = 0$ and $v = 0.04$, showing that the spacing between the vermiculite layers is not affected by the added polymer when they are collapsed by an increase in temperature. The addition of a PVME sample of molecular weight 110,000, at $v = 0.001$, had no noticeable effect on either d or T_c.

Key Words—Interlayer Spacings, Neutron Diffraction, Osmotic Swelling, Phase Transitions, Polymers, Vermiculite Gels.

INTRODUCTION

The importance and potential of the 4-component clay–polymer–salt–water system in agricultural and industrial applications could hardly be overstated, being the central problem of soil science. As pointed out by Theng (1979), "progress in our understanding of this system is at present limited more by experimental than theoretical inadequacies". Although substantial progress has been made during the past 15 years (Fleer et al. 1993), there remains a strong element of truth in this statement. We hope that the present study will contribute significantly to improving the experimental situation, by describing an investigation into the effect of adding polymers to a model clay system, the *n*-butylammonium vermiculites.

The osmotic swelling of *n*-butylammonium vermiculite in water is illustrated in Figure 1. The Figure 1a–1b process was first reported in the early 1960s (Walker 1960; Garrett and Walker 1962). It involves the absorption of large amounts of water by *n*-butylammonium vermiculite crystals placed in dilute *n*-butylammonium salt solutions, the extent of swelling being strongly dependent on the salt concentration in the soaking solution (Walker 1960). It leads to the formation of coherent gels, which show no tendency to disperse into the surrounding solution. The Figure 1b–1c process was discovered more recently (Smalley et al. 1989) and has been investigated as a function of the salt concentration c and the temperature T (Braganza et al. 1990), hydrostatic pressure P (Smalley et al. 1989), uniaxial stress along the swelling axis p (Crawford et al. 1991) and, most recently, the volume fraction r of the clay in the condensed matter system (Williams et al. 1994).

The 2 main aims of the present paper are to examine the effect of added polymers on the d-value in the gel phase (Figure 1b) and the phase transition temperature T_c between the structures of Figures 1b and 1c. Early small-angle X-ray diffraction (XRD) studies of *n*-butylammonium vermiculite gels (Norrish and Rausell-Colom 1963; Rausel-Colom 1964) showed sharp diffraction peaks for d-values in the range 8–30 nm. More recent neutron diffraction studies (Braganza et al. 1990) have confirmed the homogeneity of the swelling for d-values up to 90 nm and proved that the layers retain their orientation to a high degree in the swollen (gel) phase. Braganza et al. (1990) showed that if the temperature is raised, the gel structure (Figure 1b) collapses to give the tactoid formation (Figure 1c), where we have used the nomenclature of Kleijn and Oster (1982) to describe a structure in which

https://doi.org/10.1346/CCMN.1997.0450513 Published online by Cambridge University Press

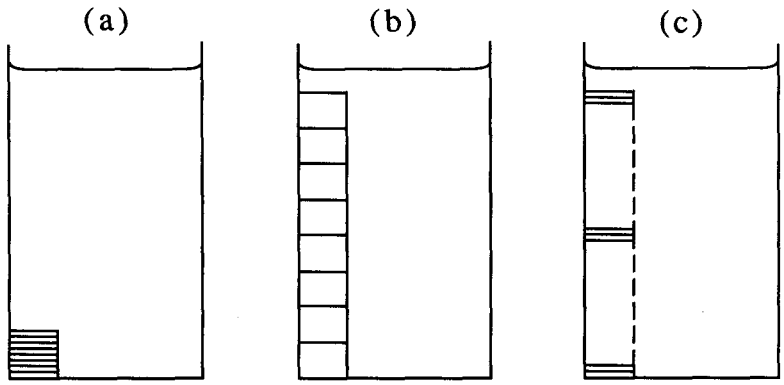

Figure 1. Schematic illustration of the swelling of *n*-butylammonium vermiculite in an 0.1 *M* *n*-butylammonium chloride solution. a) represents the *n*-butylammonium vermiculite crystal ($d \cong 2$ nm) prior to swelling, b) the gel ($d \cong 12$ nm) formed by a homogeneous 6-fold expansion at $T < 14$ °C, and c) the tactoid formed when the gel collapses at $T > 14$ °C. In (c), the dashed line represents the fact that the tactoid structure occupies the same volume as the gel structure.

groups of vermiculite layers with interlayer spacing ≅1 nm are separated by large aqueous regions with spacings in the range between 100 and 1000 nm (0.1 to 1 μm). Braganza et al. (1990) proved that the interlayer spacings within the tactoids in the case of Figure 1c were identical to those observed in the case of Figure 1a. Because of this identity we refer to the tactoid structure as having "crystalline regions". We recognize that, because of the regular interlayer spacings, the Figure 1b structure is itself a type of crystal, actually a 1-dimensional paracrystal (Williams et al. 1994), but retain the description "gel" in order to avoid confusion with the Figure 1a structure, the original crystalline vermiculite.

Adding polymers to a well-characterized clay colloid is potentially interesting both from the point of view of clay science and that of polymer science, but care is needed because the problem is a many-variable one. The 3-component clay–salt–water system has already been studied as a function of the set of variables $\{r, c, T, P, p\}$. Adding polymer to the system adds 3 new variables to be considered: the chemical nature of the polymer x, the molecular weight of the polymer M and the volume fraction of the polymer in the condensed matter system v. The variable x represents the composition of the side groups, the block structure, the stereoregularity and other features of the polymer. The symbol M represents the number-average or weight-average molecular weight of the polymer and its polydispersity. The variable v is defined as the ratio of the polymer volume to the total volume occupied by the polymer, clay, salt and water. A glossary of all the symbols used is given in Table 1.

There are therefore a total of 8 variables to be considered, creating an enormous phase space to be investigated. Our strategy was to eliminate 3 of the variables in the present study, as follows. First, attention was restricted to the unstressed systems. All experiments were carried out at $P = 1$ atm and $p = 0$: the gels were allowed to swell freely to equilibrium at atmospheric pressure. Second, attention was restricted to the case $r = 0.01$: the clay always occupied 1% of the volume in the condensed matter system. The five variables $\{c, T, x, M, v\}$ still contain a myriad of possibilities, limited only by the requirement that the polymers be water-soluble.

EXPERIMENTAL

The vermiculite crystals were from Eucatex, Brazil. Crystals about 30 mm² in area by 1 mm thick were washed and then treated for about 1 y with 1 *M* NaCl solution at 50 °C, with regular changes of solution, to produce a pure Na-vermiculite, following the procedure of Garrett and Walker (1962). The completeness of the exchange was checked from the regularity of the *c*-axis peaks in the XRD patterns, the *c*-axis spacing for the Na form being 1.49 nm. The chemical formula of the sample thus obtained was determined to be:

$$Si_{6.13}Mg_{5.44}Al_{1.65}Fe_{0.50}Ti_{0.13}Ca_{0.13}Cr_{0.01}K_{0.01}O_{20}(OH)_4Na_{1.29}$$

The unit cell weight for this formula is 807. Therefore, 807 g of this clay contains 1.29 cations, which corresponds to a cation exchange capacity (CEC) of the mineral of 160 meq/100 g. This is equal to the value obtained by Humes (1985).

To prepare the *n*-butylammonium vermiculite, the Na form was soaked in 1 *M* *n*-butylammonium chloride solution at 50 °C, with regular changes of solution, for about 1 mo. During this process, the amount of Na depleted from the crystals was determined by atomic absorption (AA) spectroscopy and was found to correspond to 1.3 monovalent cations per $O_{20}(OH)_4$ unit. Chemical analysis of the *n*-butylammonium vermiculite thus obtained showed that the amount of interlayer Na remaining was less than 1%. This confirms

https://doi.org/10.1346/CCMN.1997.0450513 Published online by Cambridge University Press

Table 1. Glossary of symbols and abbreviations used.

A_p	Area of a vermiculite surface occupied by a polymer molecule
c	Electrolyte concentration of *n*-butylammonium chloride solution
d	Average repeat distance along the swelling axis
$I(Q)$	Intensity of scattering as a function of momentum transfer
λ	Neutron wavelength
l_p	Effective thickness of an adsorbed polymer layer
LCST	Lower critical solution temperature
M	Molecular weight
M_n	Number—average molecular weight
M_w	Weight—average molecular weight
n	Power law exponent in the relation $I(Q) \propto Q^{-n}$
p	Uniaxial pressure along the swelling axis
P	Hydrostatic pressure
PAA	Poly(acrylic acid)
PEO	Poly(ethylene oxide)
PVME	Poly(vinyl methyl ether)
Q	Momentum transfer
Q_{max}	Momentum transfer at first-order diffraction maximum
r	Volume fraction of vermiculite in the condensed matter system
r_0	Unperturbed end-to-end distance of a polymer molecule
R_g	Radius of gyration of a polymer molecule
ρ	Density
SANS-J	Small-angle neutron scattering instrument at Tokai reactor
T	Temperature
T_c	Transition temperature between gel and tactoid phases
θ	Scattering angle
v	Volume fraction of polymer in the condensed matter system
W	Width of disk of vermiculite layers
x	Chemical nature of polymer
ξ	Correlation length along the swelling axis
V_{eff}	Effective volume of a polymer molecule in solution
Z_{eff}	Effective surface charge of a vermiculite layer

the accuracy of the alkylammonium ion exchange method for the characterization of clays described by Lagaly (1981). The purity was again checked by XRD, the *c*-axis spacing now being 1.94 nm. The crystals were stored in a 1 *M* *n*-butylammonium chloride solution prior to the swelling experiments.

The low molecular weight PVME used in the main study was synthesized by cationic polymerization in toluene at −78 °C with boron trifluoride etherate as initiator. The number-average molecular weight (M_n) of the PVME, measured by gel permeation chromatography (GPC) in chloroform, was 27,000 in terms of the polystyrene equivalent, and the polydispersity ratio (M_w/M_n, where M_w is the weight-average molecular weight) was 1.40. Experiments on PVME samples with narrow molecular weight distributions ($M_w/M_n < 1.1$) in the molecular weight range between 500 and 4000 have shown that the absolute value of M_n obtained by ^{1}H NMR is equal to 0.67 times the polystyrene equivalent value obtained by GPC (Sawamoto and Kamigaito 1995). If we assume that this factor holds for our sample, although it may depend on the GPC conditions (such as temperature, kind of column used and solvent) and the polymer structure (such as stereoregularity), then the true value of M_n would be 18,000, corresponding to a degree of polymerization of 310.

The high molecular weight PVME was obtained by fractionation of a polydisperse sample purchased from Scientific Polymer Products, Inc. (6265 Dean Parkway, Ontario, New York 14519). It had a polystyrene equivalent M_n of 1.64×10^5 ($M_w/M_n = 1.05$), which on the basis of the assumption used above would correspond to a true value of M_n of 110,000. The PEO was also purchased from Scientific Polymer Products, Inc., with manufacturers specifications $M_w = 10{,}900$ and $M_n = 9200$, and the PAA was purchased from Polymer Laboratories Ltd. (Separation Science Division, Essex Road, Church Stretton, Shropshire SY6 6AX, United Kingdom), with manufacturers specifications $M_w = 28{,}000$ and $M_n = 18{,}000$ ($M_w/M_n = 1.6$). Both of these samples were used without further purification.

The main study was of the vermiculite–PVME system. We note that the PVME–water system has itself an interesting (v, T) phase diagram of lower critical solution temperature (LCST) type (Tanaka 1993). For a PVME sample of weight-average molecular weight 98,000, the phase separation temperature between PVME and water occurs at 33.0 ± 0.2 °C in the v range between 0 and 0.1 (Tanaka 1993). This was slightly above the highest temperature studied with our high molecular weight PVME (32 °C) and for the lower molecular weight PVME we used, the LCST is

https://doi.org/10.1346/CCMN.1997.0450513 Published online by Cambridge University Press

shifted to higher temperatures, well above the range of interest here. The PVME and water were therefore miscible over the temperature range of the present study.

Solutions of the required volume fraction of PVME (or other polymer) were prepared by dissolving a known mass of the polymer (ρ = 1.03 g/cm^3 for PVME) in a known volume of a 0.1 molar (or 0.01 *M*) *n*-butylammonium chloride solution, itself prepared by dissolving a known mass of *n*-butylammonium chloride in D_2O. It was necessary to swell the crystals in D_2O rather than H_2O solutions because of the large incoherent scattering cross section of hydrogen which would otherwise have obscured the scattering of interest.

Prior to the swelling experiments, the crystals were washed thoroughly to remove any molar *n*-butylammonium chloride solution that may have been trapped in surface imperfections. This was achieved by rinsing the crystals with 500 cm^3 of distilled water at 60–80 °C 15 times before drying on filter paper. The distilled water was heated in order to prevent any swelling occurring during this washing process since, although the absorption of distilled water is rapid, it does not occur above 40 °C, as this is above the phase transition temperature for tactoid formation (Williams et al. 1994). After drying, the crystals were cut to dimensions of approximately 0.5 × 0.5 × 0.1 cm. These were individually weighed and the volume of a crystal in its fully hydrated state calculated using the density (ρ = 1.86 g/cm^3). After weighing, a single vermiculite crystal was placed into a quartz sample cell of dimensions 1 × 1 × 4.5 cm and an appropriate amount of the polymer and *n*-butylammonium chloride solution (typically 2.5 cm^3) was added to prepare an r = 0.01 sample. The cells were then sealed with parafilm and allowed to stand at 7 °C for 2 weeks prior to the neutron scattering experiments, to ensure that full equilibrium swelling had been achieved (Williams et al. 1994).

The neutron diffraction experiments were carried out at the JRR-3M Research Reactor, Japan Atomic Energy Research Institute (JAERI), Tokai-mura, using the SANS-J instrument. A monochromatic beam of neutrons was used and the incident beam was collimated by passage through a 5-mm diameter circular aperture. The samples were mounted on a temperature-controlled 4-position sample changer under the control of the instrument computer. Neutrons scattered by the gel samples were recorded on a 2-dimensional area detector, with 128 × 128 pixels, situated behind the samples. In a typical experiment, neutrons of wavelength λ = 0.6 nm and a sample to detector distance of 1.5 m were used, covering the approximate Q-range between 0.2 and 2 nm^{-1}, where the wave number Q is defined by the equation:

$$Q = \left(\frac{4\pi}{\lambda}\right)\sin\left(\frac{\theta}{2}\right) \qquad [1]$$

with θ the scattering angle. In some experiments, neutron wavelengths of λ = 0.357 nm or λ = 0.685 nm and sample-to-detector distances of 2.5, 4.0 or 10.0 m were used to vary the Q-range of the instrument.

The quartz sample cells used were practically transparent to neutrons at all the wavelengths utilized on SANS-J and the small-angle neutron scattering from D_2O was of low intensity and completely unstructured over the Q-ranges studied. All of the sample runs were corrected for the background scattering arising from the cell and D_2O; after making the appropriate transmission corrections, the scattering arising from a cell containing D_2O was subtracted from the sample runs. In this way the scattering patterns analyzed arose purely from the gels.

A preliminary core study was performed using 3 polymers in the molecular weight range 10,000 to 30,000, PVME, PEO and PAA, at a polymer volume fraction of v = 0.01. In addition to holding M (approximately) and v constant, attention was restricted to c = 0.1 M and 0.01 M and temperatures in the vicinity of T_c in order to determine the x-dependence of the effect. The x = PVME, M = 18,000 system was then chosen for a detailed study of the v-dependence at c = 0.1 M. Finally, at a fixed small volume fraction, v = 0.001, the M-dependence in the PVME system was investigated at c = 0.1 M and 0.01 M by measuring d and T_c for a sample with M = 110,000. Our study of the salt concentration, temperature, polymer nature, volume fraction and molecular weight dependence of the behavior of the system is far from exhaustive, but this is necessarily so for a 5-variable problem.

RESULTS

Study of PVME-, PEO- and PAA-Substituted Gels at v = 0.01, c = 0.1 M

Three types of polymer in the molecular weight range between 10,000 and 30,000 were studied at a polymer volume fraction of 1%. Before adding polymer, it was necessary to check the properties of the new batch of vermiculite samples and the performance of the instrument by studying the [c, T] behavior of the system with no added polymer. Since the [c, T] behavior of the pure aqueous system has already been extensively studied by neutron scattering (Braganza et al. 1990; Williams et al. 1994), attention was restricted to c = 0.1 M and 0.01 M and temperatures in the vicinity of the phase transition temperature T_c. The c = 0.01 M study is described later.

First, 4 pure aqueous c = 0.1 M gels were studied at T = 8 °C. The scattering patterns observed on the 2-dimensional multidetector were reproducible from sample to sample and an example is shown in Figure 2a, where Figure 2d shows the geometry of the scattering experiments. The samples were mounted with

https://doi.org/10.1346/CCMN.1997.0450513 Published online by Cambridge University Press

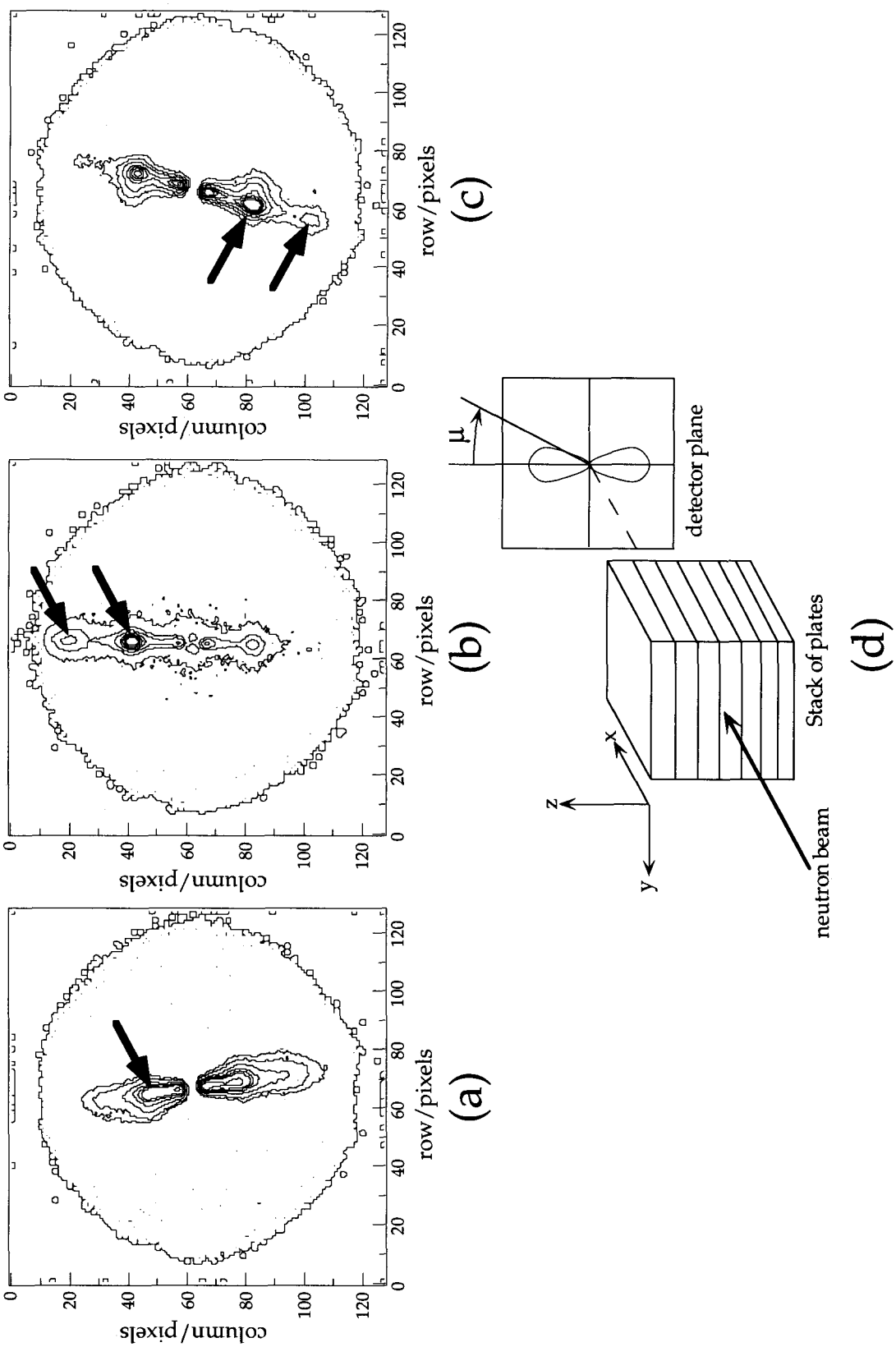

Figure 2. Contour plots of typical neutron scattering patterns for $r = 0.01$, $c = 0.1$ *M* gels at $T = 8$ °C. The numbers show the pixel code. a) No added polymer. The arrow marks the first-order diffraction maximum at $Q_{max} = 0.52$ nm^{-1}. b) With 1% PVME. The arrows mark the first maximum at $Q_{max} = 0.67$ nm^{-1} and the second maximum at $Q_{max} = 1.34$ nm^{-1}. c) With 1% PEO. The arrows mark the first maximum at $Q_{max} = 0.70$ nm^{-1} and the second maximum at $Q_{max} = 1.40$ nm^{-1}. d) The geometry of the scattering experiments.

https://doi.org/10.1346/CCMN.1997.0450513 Published online by Cambridge University Press

the clay layers horizontal to the ground and the scattering pattern consists of 2 lobes of intensity above and below the plane of the layers in the gel, defined as the *xy*-plane in Figure 2d. If the layers were perfectly parallel then coherent scattering would only occur along the *z*-axis perpendicular to the layers, but in reality there are defects in the gel, so scattering occurs to either side of this axis such that almost all of the scattering falls within 2 cones of 60° azimuthal width above and below the horizontal plane, corresponding to $\mu = 30°$ in Figure 2d.

The slight tilting of the line of most intense scattering from the *z*-axis in Figures 2a and 2b and the asymmetries in the cones of scattering in the $+z$ and $-z$ directions are due to the average orientation of the stack of layers lying slightly out of the *xy*-plane in the sense of rotations about the *x*-axis and *y*-axis, respectively. The existence of intensity maxima within the cones is due to a pronounced interference effect between the vermiculite layers, which have a well-defined interlayer spacing.

The scattering from the polymer-added systems, also taken for 4 samples of each type of added polymer, was also reproducible. An example of the scattering from a $c = 0.1$ *M* PVME sample is shown in Figure 2b and that from a $c = 0.1$ *M* PEO sample shown in Figure 2c. The first remarkable feature of these patterns is that the cones of scattering have become narrower than those observed in the pure aqueous system, almost all of the scattering now lying within $\mu = 25°$, rather than the 30° observed previously. This effect was observed for all the polymer-added samples studied in the gel phase. Since the width of the cone is a measure of the orientation distribution of the vermiculite layers with respect to the *z*-axis and therefore a measure of the parallelity of the stack, this shows that: 1) *the addition of polymer causes the vermiculite layers to become more parallel in the gel phase.* The second remarkable feature of Figures 2b and 2c is that the diffraction lobe has shifted to higher Q as compared with the pure aqueous $c = 0.1$ *M* sample. This means that 2) *the addition of polymer causes a decrease in the interlayer spacing between the vermiculite layers in the gel phase.* This is shown more clearly by sector-summing the data, by taking constant Q cuts within the appropriate azimuthal cones, to give plots of $I(Q)$ vs. Q, as shown in Figure 3.

Similar patterns to those shown in Figures 2 and 3 were observed for all samples in the gel phase. In order to extract the most precise information from the neutron diffraction patterns it would be necessary to analyze them quantitatively using a 1-dimensional paracrystalline lattice model (Shibayama and Hashimoto 1986). Although such an analysis can be performed for small-angle XRD patterns from vermiculite gels (Rausell–Colom et al. 1989), it is not so straightforward for small-angle neutron scattering data because of the poorer resolution due to the larger size of the beam and the wider spectral distribution, $\Delta\lambda/\lambda \cong 0.1$. However, the sharpness of the diffraction effect permits an immediate approximate evaluation of the *d*-value by measuring Q_{max}, the Q-value at the maximum of the first order diffraction peak, and applying the simple equation:

$$d = 2\pi/Q_{max} \quad [2]$$

Although this procedure is not strictly rigorous, we note that in all cases when we were able to observe a second-order diffraction peak, the position of this peak was equal to twice the value of Q_{max} for the first-order diffraction peak, to the limit of experimental error. This validates the approximate evaluation, since it shows that the form factor of the scattering object has a negligible influence on the peak positions, and it was applied to all the $I(Q)$ vs. Q plots obtained.

The plot of the pure aqueous data in Figure 3 (the crosses) shows an interference maximum at $Q_{max} = 0.52$ nm^{-1}, corresponding to $d = 12$ nm, in excellent agreement with the literature value (Previous observations have all fallen within the range between 11 and 14 nm, with a weighted average of $d = 12$ nm). Four samples were run at this set of conditions ($c = 0.1$ *M*, $T = 8$ °C) and the constancy of the position of the interference maximum confirmed that there is excellent sample to sample reproducibility in the system. The scattering from the PVME sample, shown by the squares in Figure 3, has a very strong first-order maximum at $Q_{max} = 0.67$ nm^{-1}, corresponding to $d = 9.4$ nm and that from the PEO sample, shown by the circles in Figure 3, has a strong first-order maximum at $Q_{max} = 0.70$ nm^{-1}, corresponding to $d = 9.0$ nm. It is noteworthy from the insets in Figure 3 that both types of polymer-added sample exhibit fairly strong second-order diffraction effects, which is rare for a pure aqueous sample. This means that 3) *the addition of polymer causes the vermiculite layers to be more regularly spaced in the gel phase.*

Whether or not results (1)–(3) would apply to the PAA-added samples is unknown, because *the samples with added PAA did not swell at all* in $c = 0.1$ M, $v = 0.01$ PAA solutions. Indeed, crystals placed in $v = 0.01$ PAA solutions did not swell in water irrespective of the salt concentration c, even in solutions with no added salt. *The addition of PAA therefore stabilizes the crystalline phase*, illustrated in Figure 1a, and all subsequent results refer to the neutral polymers.

For the pure aqueous samples and those containing neutral polymers, the tactoid phase was stable at higher temperatures. The effect of added polymer on the temperature-induced phase transition was investigated by studying the scattering patterns shown in Figure 3 as a function of temperature. The scattering from the pure aqueous sample is shown in Figure 4a. It is clear

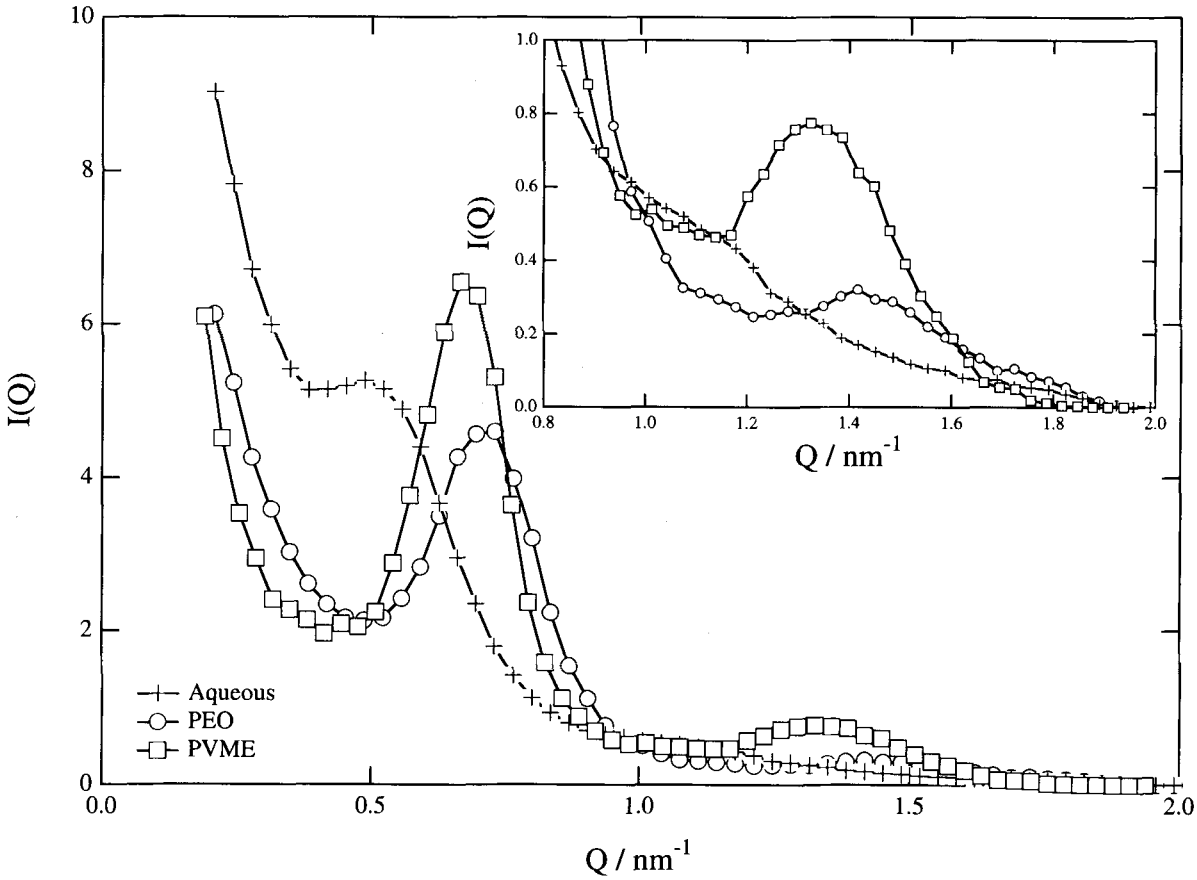

Figure 3. The sector averaged plots of the patterns shown in Figure 2 for r = 0.01, c = 0.1 M gels at T = 8 °C. The crosses, squares and circles denote the scattering from the pure aqueous system and those with 1% PVME and 1% PEO, respectively. The insets are the scattering on a magnified (×5) intensity scale, showing the clear second-order diffraction maxima for the polymer-added samples.

that the interference effect collapses between 12.7 and 13.8 °C. The disappearance of the gel peak in the neutron scattering patterns has previously been used to define T_c for the pure aqueous system (Smalley et al. 1989; Braganza et al. 1990; Williams et al. 1994). Although our recent more detailed XRD study of the phase transition indicates that this definition is only an approximate one, it is adequate for our present purposes. In this case it gives T_c = 13.3 ± 0.6 °C, in good agreement with the literature value. Note that the shape of the small-angle scattering also changes when the sample is heated to above T_c, as described below. The complete reversibility of the transition was confirmed by recooling the sample to 8 °C, then reheating it to 17 °C and recording the scattering. The patterns were identical to those obtained previously at these temperatures. The scattering patterns from the PVME samples at 8 and 17 °C are shown in Figure 4b and those from the PEO samples at the same temperatures are shown in Figure 4c. It is clear that the same type of dramatic change in scattering takes place over this temperature range in the polymer-added samples, and scans at intermediate temperatures showed that 4) *the addition of neutral polymer has no effect on the phase transition temperature between the tactoid and gel phases of the vermiculite system.*

The signature of the crystalline regions in the tactoid phase of the pure aqueous system is a first-order diffraction peak at Q = 3.24 nm^{-1} (Braganza et al. 1990), corresponding to a d-value of d = 1.94 nm. The patterns shown in Figure 4 were obtained with λ = 0.685 nm and sample-to-detector distances of 4 m (Figure 4a), and 1.5 m (Figures 4b and 4c), for which this peak lies beyond the Q-range of the instrument. At the shortest available wavelength on SANS-J, λ = 0.357 nm, and the shortest possible sample-to-detector distance of 1.5 m, we were able to observe the tail of the first-order diffraction peak of the crystalline regions in the pure aqueous system as an upturn in the scattering at the edge of the multidetector, as shown by the crosses in Figure 5. This upturn in the scattering at the edge of the Q-range was observed to be the same for the pure aqueous, PVME-added and PEO-added samples, as shown respectively by the crosses,

https://doi.org/10.1346/CCMN.1997.0450513 Published online by Cambridge University Press

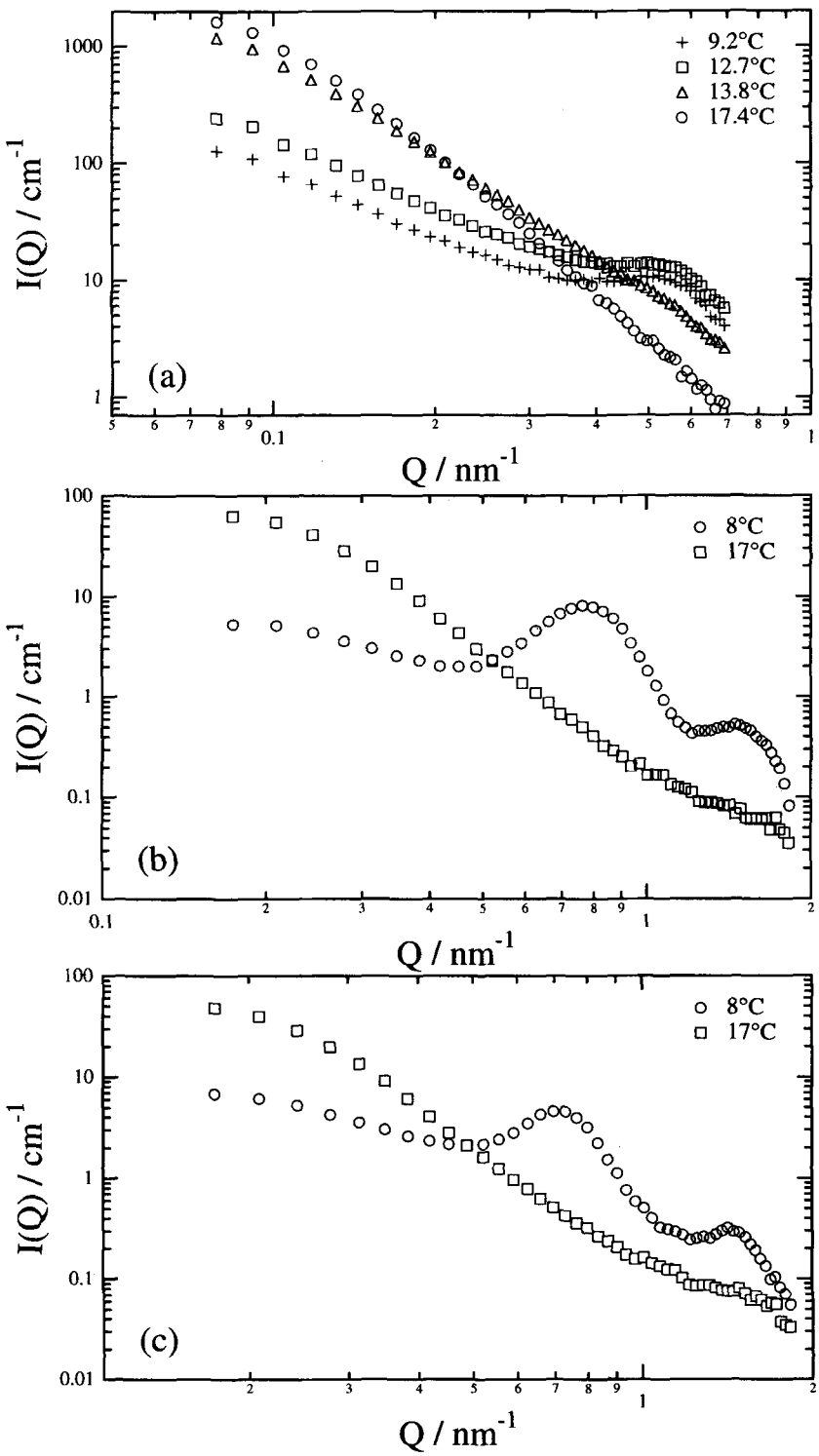

Figure 4. a) The temperature-induced phase transition in the c = 0.1 M pure aqueous system for a sample with T_c = 13.3 ± 0.6 °C. The intensity has been plotted on a logarithmic scale to emphasize the difference in the small-angle scattering. b) and c) The patterns obtained a few degrees either side of T_c for c = 0.1 M PVME-added and PEO-added samples, respectively, on a logarithmic intensity scale.

https://doi.org/10.1346/CCMN.1997.0450513 Published online by Cambridge University Press

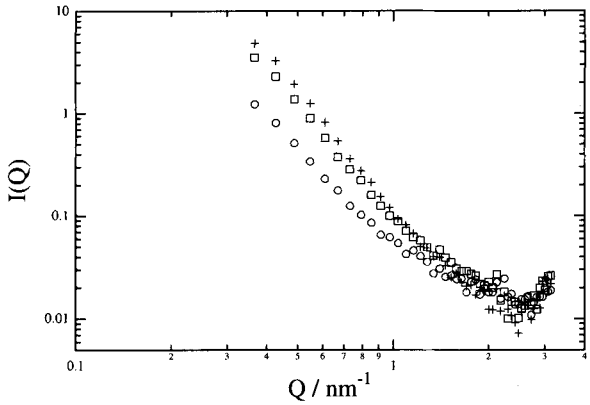

Figure 5. The upturn in the scattering at higher Q in the tactoid phase, at 25 °C. The sample-to-detector distance was 1.5 m and the wavelength $\lambda = 0.357$ nm. The crosses, squares and circles denote the scattering from the pure aqueous system and those with 1% PVME and 1% PEO, respectively.

squares and circles in Figure 5. Our XRD studies of the pure aqueous and PVME-added systems at higher Q values have confirmed that the crystalline peak position is unaffected by added polymer, so 5) *the spacing between the vermiculite layers is not affected by the added polymer when they are collapsed by an increase in temperature.*

Study of PVME-, PEO- and PAA-Substituted Gels at $v = 0.01$, $c = 0.01$ M

Similar experiments to those described above were carried out at $c = 0.01$ M. As before, the PAA-added samples did not swell. In the pure aqueous system, a weak interference effect was observed at $Q = 0.19$ nm^{-1}, corresponding to a d-value of $d = 33$ nm, and the scattering changed profoundly between 29 and 31 °C, corresponding to a phase transition temperature $T_c = 30 \pm 1$ °C. Both the values for d and T_c were again in good agreement with the literature values and the phase transition was again proved to be completely reversible by recooling to 17 °C and showing the scattering to be identical to that obtained previously at this temperature.

The almost perfect sample-to-sample reproducibility of the 0.1 M samples and the good agreement with the published results for d and T_c at both $c = 0.1$ M and $c = 0.01$ M showed that any differences we observed in the properties of the systems with added polymer were genuine effects. However, at $c = 0.01$ M we were only able to study 2 PVME-added and 2 PEO-added samples, so we did not obtain statistically significant information on the effect of added polymer on the d-values at this salt concentration. All 4 polymer-added samples gave weak interference maxima in the Q-range between 0.18 and 0.20 nm^{-1}, corresponding to d-values in the range between 31 and 35 nm. This is insignificantly different to the value obtained for the pure aqueous system, so the effect is probably a weak one. The 2 samples giving the clearer diffraction traces were chosen for an investigation of T_c, which is much less sensitive to sample-to-sample variability than d (Williams et al. 1994). The temperature-dependent scans obtained from the $c = 0.01$ M PVME samples are shown in Figures 6a and those for the PEO samples in Figure 6b. In both cases $T_c = 28 \pm 1$ °C, compared with $T_c = 30 \pm 1$ °C for the $c = 0.01$ M pure aqueous system. This again indicates that the addition of polymer causes only a slight change in the properties of the system at $c = 0.01$ M, and reinforces result (4) obtained at $c = 0.1$ M.

Study of the (v, T) Behavior of the $c = 0.1$ M PVME–18,000 System

Since the addition of PEO and PVME had very similar effects, it seemed logical to continue work with 1 system at the expense of the other. We decided to continue work with the PVME system as our neutral polymer system, as this one has extra interest because of the PVME–water phase separation which occurs in the absence of clay at higher temperatures (Tanaka 1993). The main development was to systematically investigate the effect of the volume fraction of PVME on both d and T_c for the $r = 0.01$, $c = 0.1$ M system. The details of this investigation have been reported previously (Jinnai et al. 1996), so we proceed directly to the results, which are given in Table 2. The average d-values obtained have been plotted as a function of the volume fraction, expressed as a percentage, in Figure 7.

The number of samples studied in each case was between 3 and 8, and the complete set of results obtained is given in the second column of Table 2. The d-values for the polymer-added samples were very consistent from sample to sample, with the exception of the 4% PVME samples, where 2 separate groups of results with d-values of approximately 9 and 6.5 nm gave rise to an average value of 7.7 nm. The variation of the average d-value with the volume fraction seems to be well represented by the exponential fit shown by the dotted line in Figure 7, where the error bars represent ±10% of the average values obtained, due to sample-to-sample variability. The exponential fit is characterized by:

$$d = 7.9 + 3.9 \exp(-1.0v) \qquad [3]$$

where d is expressed in nm and v is expressed as a percentage. The correct limit of $d \cong 12$ nm is obtained for the pure aqueous system and the value $d \cong 8$ nm is obtained as the limiting result for high polymer volume fractions.

The decrease in the d-value with increasing amount of polymer in the system is an interesting result, as it has been reported that the interlayer spacing of clay–polymer complexes generally increases with the

https://doi.org/10.1346/CCMN.1997.0450513 Published online by Cambridge University Press

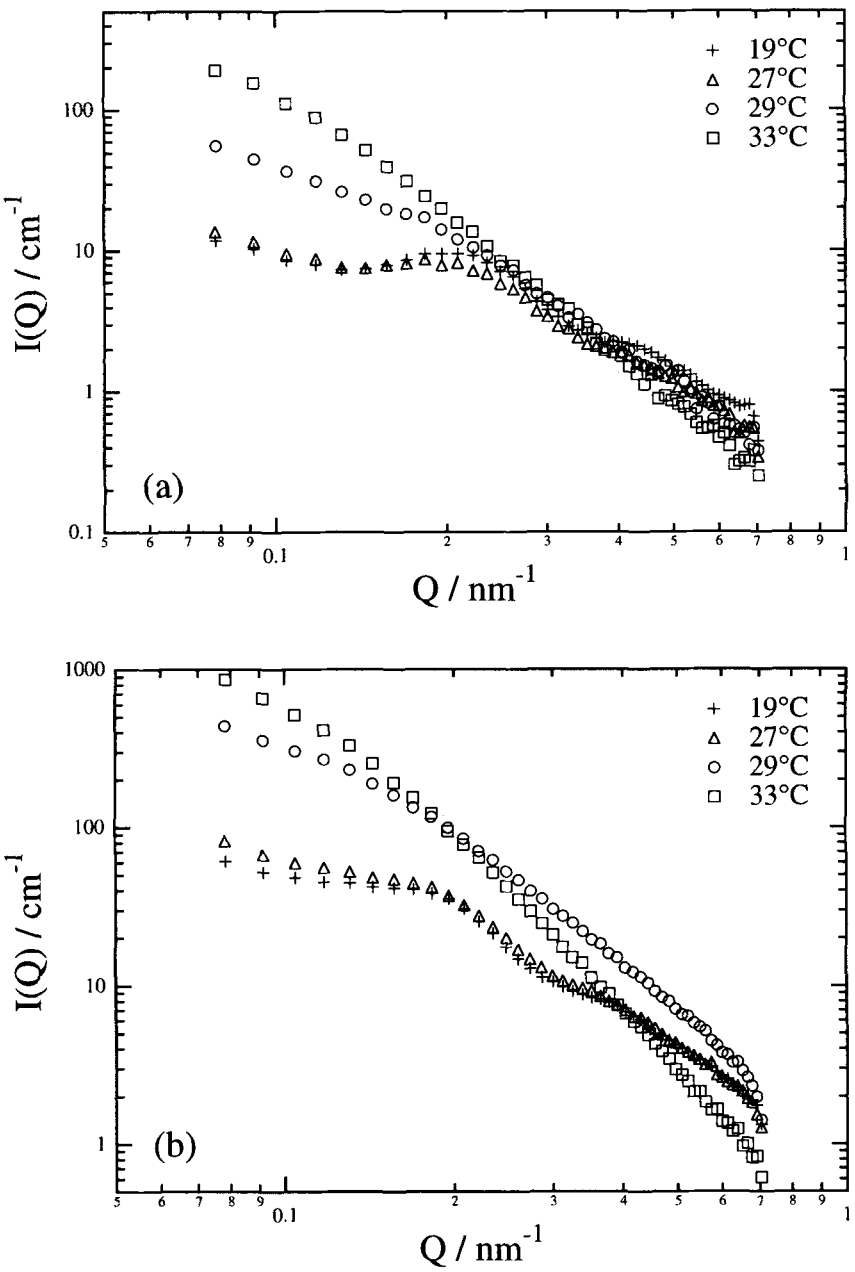

Figure 6. The temperature-induced phase transition in the c = 0.01 M polymer-added systems, a) with 1% PVME and b) with 1% PEO. T_c = 28 °C in both cases.

Table 2. The values of d and T_c obtained for the PVME-18,000 system.

v %	All d-values observed (nm)	d (nm)	T_c (°C)
0	13.2, 11.6, 12.3, 12.0, 13.7, 12.3	12.5	14
0.1	11.5, 10.3, 10.3	10.7	15
0.2	11.5, 10.3, 11.1, 10.7	10.9	14
0.4	10.3, 10.3, 10.7, 10.7	10.5	14
1.0	9.9, 9.4, 9.0, 9.2, 9.1, 9.1	9.3	14
2.0	9.0, 8.3, 8.3, 9.0, 9.0	8.7	15
4.0	8.6, 9.0, 9.0, 9.0, 6.2, 6.7, 6.4, 6.9	7.7	15

amount of polymer adsorbed (Theng 1979). However, the observations reviewed by Theng (1979) were for interlayer spacings in the range between 1 and 3 nm, which corresponds to the crystalline regions in the tactoid phase of our system. By contrast, we have observed no expansion of the tactoids by added polymers, only the contraction of the gel phase. Possible mechanisms for this contraction are discussed later. It is also noteworthy from the fourth column of Table 2 that T_c was always observed to be within the range

https://doi.org/10.1346/CCMN.1997.0450513 Published online by Cambridge University Press

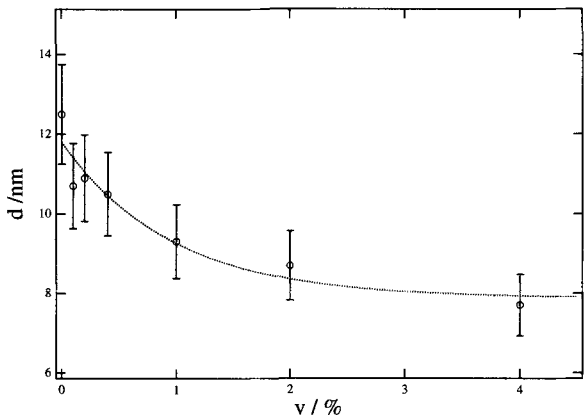

Figure 7. The average *d*-value (nm) as a function of the PVME volume fraction for $r = 0.01$, $c = 0.1$ *M*, $T = 8$ °C.

between 13 and 16 °C irrespective of the volume fraction of PVME in the system. This substantiates our conclusion that the addition of polymer has no effect on the phase transition temperature between the tactoid and gel phases of the vermiculite system. In view of the 50% contraction observed in the *d*-value of the gel phase, this is another conspicuous result.

Asymptotic Behavior of the Scattering at Low Q

One of the interesting features of Figures 4 and 6 is that there seems to be a difference in the shape of the small-angle scattering accompanying the collapse of the gel peak. The traces shown in Figures 4 and 6 were obtained at sample-to-detector distances of 1.5 and 4 m, the approximate Q-ranges being 0.2 to 2.0 nm^{-1} and 0.07 to 0.7 nm^{-1}, respectively. In the former Q-range (henceforth referred to as a higher Q scan), we are sensitive to interference effects from spacings in the range between 3 and 30 nm, ideal for observing the diffraction arising from the interlayer spacing of the $c = 0.1$ *M* gels. The scattering at lower Q was obtained from the same samples at a sample-to-detector distance of 10 m, the approximate Q-range being 0.03 to 0.3 nm^{-1} (henceforth referred to as a lower Q scan). The lower Q scan and the higher Q scan obtained from the same pure aqueous sample at $T = 9.5$ °C are shown as the crosses in Figure 8a and the scans at $T = 16.2$ °C are shown by the crosses in Figure 8b. The lower Q scattering was investigated as a function of volume fraction for the PVME-18,000 system and examples of the patterns obtained for a polymer-added sample are shown by the circles in Figures 8a and 8b, which show the complete Q scans for a 1% PVME-18,000 sample at $T = 9.5$ °C and $T = 16.2$ °C, respectively. It is clear from these plots that the lower Q and higher Q scans sew together well both in terms of the magnitude of the intensity and the gradient in the region where they overlap, around $Q = 0.2$ nm^{-1}.

A preliminary analysis of the lower Q data was carried out by plotting the logarithm of the scattering intensity against the logarithm of Q. These plots were approximately linear, showing that the low Q scattering could be characterized by the equation $I(Q) \propto Q^{-n}$. The power-law exponent n obtained by least-squares fits to the data have been collected in Table 3, (a) in the gel phase and (b) in the tactoid phase. The main feature of Table 3 is that there appears to be no systematic variation of the gradients with respect to the volume fraction of PVME. The gradients have therefore been averaged over all samples, with the exception of the tactoid phase result for the pure aqueous system. The latter appears anomalous, but we do not have the statistics to say whether or not this is a real effect. The results show that the log–log plots do have significantly different gradients in the gel and tactoid phases, that in the gel phase corresponding to the approximate relationship $I(Q) \propto Q^{-2.5}$ and that in the tactoid phase to $I(Q) \propto Q^{-2}$.

Quantitative analysis of the asymptotic behavior at low Q is in progress and will be discussed elsewhere. Here we give only a very qualitative interpretation. If ξ represents the longitudinal correlation or coherence length of the layers along the swelling axis and W represents the lateral width of the layers, then the assembly of the layers will behave as an infinitely thin disc if $\xi \ll 2\pi/Q \ll W$, where $2\pi/Q$ is the length scale with which we probe the structure of the layers. In these circumstances, the scattering intensity will be given by $I(Q) \propto Q^{-n}$ with $n = 2$, as observed in the tactoid phase. If $\xi \leq 2\pi/Q \ll W$, the effect of the finite thickness of the disc becomes important, which makes n greater than 2 (for example, 2.5, as observed in the gel phase). Since we may expect the correlation length ξ to be short in the tactoid phase and to increase dramatically upon gel formation, the behavior is qualitatively explicable.

Study of Molecular Weight Dependence in the PVME System

The effect of adding a polymer of much higher molecular weight, namely a PVME sample with $M_n \approx 100{,}000$, was investigated at $c = 0.1$ *M* and 0.01 *M*. There was very little PVME-100,000 available, so it was only possible to prepare 2 samples at each salt concentration, both at a volume fraction of 0.1% polymer. The 2 $c = 0.1$ *M* gels both gave a first-order diffraction peak at $Q_{max} = 0.48$ nm^{-1}, corresponding to a *d*-value of 13 nm, approximately the same as that observed in the pure aqueous system. The gradients of the log–log plots of the lower Q scattering were again the same, and T_c was again 14–15 °C, showing that the addition of a small quantity of a high molecular weight polymer had no observable effect on the $c = 0.1$ *M* vermiculite system. Similar results were obtained for the $c = 0.01$ *M* gels. It is noteworthy that

https://doi.org/10.1346/CCMN.1997.0450513 Published online by Cambridge University Press

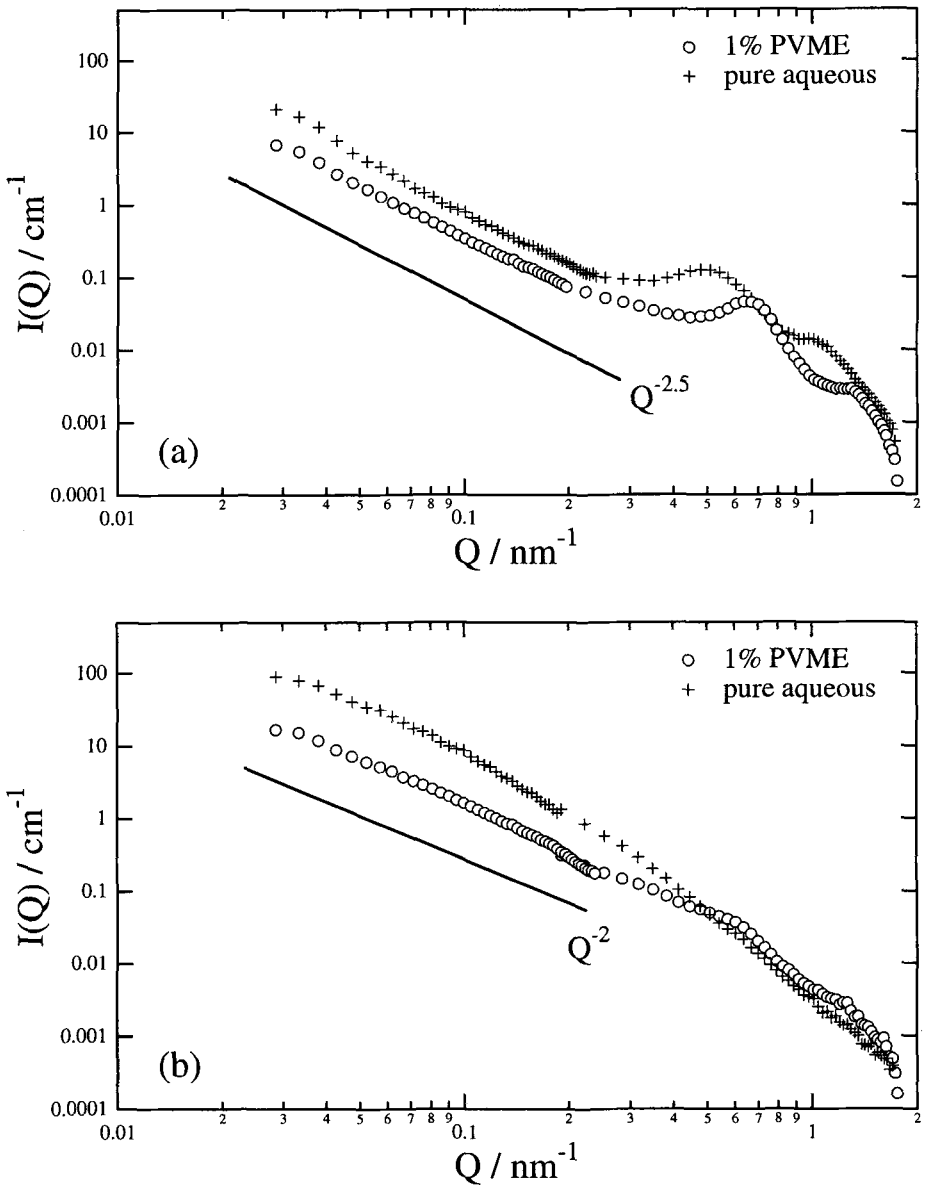

Figure 8. The complete Q scans obtained a) at T = 9 °C and b) at T = 16 °C, in the gel phase and tactoid phase, respectively, on logarithmic intensity and Q scales. The crosses and the circles denote the scattering from the pure aqueous and 1% PVME-added samples, respectively, and the straight lines indicate the approximate gradients of the low Q scattering in each phase. Note that with T_c = 15 °C the tactoid phase results are near to T_c and there is evidence for weak persistence of the gel peak around Q = 0.7 nm^{-1} in the diffraction trace from the PVME-added sample at 16 °C.

none of the neutral polymers had any observable effect on either d or T_c at c = 0.01 M.

DISCUSSION

Sizes of Polymer Molecules

In discussing the possible mechanisms for our results, it is useful to have an estimate of the sizes of the polymer molecules used. Brandrup and Immergut (1989) give the unperturbed end-to-end distance r_0 of a PVME chain as:

$$r_0 = 900\ M^{1/2} \times 10^{-4}\ \text{nm} \qquad [4]$$

Inserting M = 18,000 into this formula gives $r_0 \cong 12$ nm, and dividing this number by $\sqrt{6}$ gives the radius of gyration $R_g \cong 5$ nm, as shown in the first row of Table 4. Utilizing similar formulae for the PEO and PAA chains enables us to complete Table 4, where the r_0 and R_g values have been given to 2 significant figures, the limit of the accuracy in the molecular weight determinations.

https://doi.org/10.1346/CCMN.1997.0450513 Published online by Cambridge University Press

Table 3. The power-law exponents n in the relation $I(Q) \propto Q^{-n}$ obtained in the lower Q SANS experiments.

v (%)	(a) Gel phase	(b) Tactoid phase
0	2.55	2.55
0.1	2.63	N.A.
0.2	2.40	N.A.
0.4	2.27	N.A.
1.0	2.36	2.16
2.0	2.55	2.08
		2.12
4.0	2.60	2.14
		2.06
Average	2.48	2.11

The gradients were obtained in the Q-range 0.03 $nm^{-1} < Q < 0.2$ nm^{-1}. (a) Gel phase (8 °C $< T <$ 11 °C), (b) tactoid phase (16 °C $< T <$ 18 °C). The average in (a) was taken over all samples. The average in (b) was taken over the polymer-added samples only. The lower Q scattering from the tactoid phase was measured for 2 samples at v = 2% and 4%, but not measured at v = 0.1%, 0.2% and 0.4%. N.A. is an abbreviation for not available.

One thing that is immediately apparent from Table 4 is that the marked difference in behavior between the neutral and charged polymer systems is not a steric effect. Both the PVME-18,000 and PAA-28,000 chains have radii of gyration of approximately 5 nm. Since the d-value of 12 nm in the pure aqueous system at c = 0.1 M is composed of a vermiculite layer of approximate thickness 1 nm and an interlayer spacing of approximate thickness 11 nm, it would seem that both polymer chains should be able to "fit" into the vermiculite gels. The stabilization of the crystalline phase in the PAA-added system is therefore definitely attributable to the charge on the polymer chain. The PAA polymer can be regarded as a prototype for the humic acids that are the major polymer constituent in soils, so the strong effect it has on the clay system could have considerable implications in soil science. However, the interactions between charged polymers and charged surfaces are considerably more complicated than those between neutral polymers and charged surfaces (Theng 1979) and in the following we restrict attention to the PVME and PEO systems.

There are 3 immediately obvious sites for a polymer molecule in and around the vermiculite gel: (A) adsorbed onto the surface of a single plate, in a flattened configuration, (B) as free chains inside the gel phase and (C) as free chains in the supernatant fluid surrounding the gel. The approximate matching of the size of the polymer to the interlayer separation in certain cases suggests another possibility, that the PVME or PEO molecules could act (D) as bridges between the vermiculite layers, adsorbed onto the surfaces of 2 neighboring layers. These 4 possibilities suggest various mechanisms for the d vs. v plot shown in Figure 7. The obvious ones are that the gel is compressed either by osmotic pressure due to an excess of polymer molecules in the supernatant fluid or by an electrical effect due to type (A) adsorption being accompanied by a redistribution of charge within the gel, affecting the layer–layer interaction. Other mechanisms are possible. For example, the addition of polymer to the system could perturb the distribution of salt between the gel and the supernatant fluid (Williams et al. 1994), again affecting the layer–layer interaction.

Table 4. The sizes of the polymer molecules used.

Polymer	M_n	r_0 (nm)	R_g (nm)
PVME	18,000	12	4.9
PVME	110,000	30	12
PEO	9,200	7.2	2.9
PAA	28,000	12	5.1

Osmotic Pressure Due to Excess Molecules in the Supernatant Fluid

Let us first consider the free chains. Results (1) to (3) are compatible with the site population being (C) > (B). In these circumstances, the excess of polymer molecules in the supernatant fluid, as compared with the fluid in the gel phase, would exert an osmotic pressure on the gel and the effect should be similar to that of applying an external pressure to the gel. The effects of 2 different types of pressure on *n*-butylammonium vermiculite gels have been studied by neutron scattering (Smalley et al. 1989; Crawford et al. 1991). The application of hydrostatic pressure, when the whole condensed matter system is compressed uniformly from outside, has an effect quite different from what we have observed for the polymer addition; the phase transition temperature changes but the d-value within the gel phase remains approximately constant (Smalley et al. 1989). However, the effect of uniaxial stress on the gels, when a piston inside the condensed matter system compresses a gel along its swelling axis, causes the diffraction patterns to sharpen and the d-value to decrease (Crawford et al. 1991), just as we have described here. Indeed, the d-value also decreases exponentially as a function of uniaxial stress (Crawford et al. 1991), so the analogy of polymer volume fraction v to uniaxial pressure p is an attractive one.

Although osmotic pressure may make a contribution to the decrease in d-value we have observed at c = 0.1 M, when the interlayer spacing is about 10 nm, the results show that strong fractionation of polymers into the supernatant fluid cannot occur when the interlayer spacing is about 30 nm. We studied 2 PVME-18,000-added gels and 2 PEO-added gels under these conditions and saw no evidence for any compression. Although there are insufficient statistics to prove the point for one individual system, we note that the PEO has a molecular weight approximately one-half that of the PVME–18,000, so there should be twice as many PEO molecules present at a given volume fraction, in-

https://doi.org/10.1346/CCMN.1997.0450513 Published online by Cambridge University Press

tensifying the effect, leading to yet smaller d-values for strong fractionation at $c = 0.01$ M. The insensitivity of the d-value for the 4 polymer-added samples studied under these conditions therefore suggests (C) $\approx$ (B) at the larger interlayer spacing studied. Since the $c = 0.01$ M gels are more compressible than the $c = 0.1$ M gels (Crawford et al. 1991), this further suggests that osmotic pressure is probably not the leading effect in the decrease in d-value observed at $c = 0.1$ M. It therefore appears that the polymers have some effect inside the gel. The most likely source of this effect is polymer adsorption onto the surfaces of the vermiculite layers.

Polymer Adsorption onto the Vermiculite Surface

In order to estimate the degree of polymer adsorption, we first calculate the total layer surface area of the vermiculite clay in the swollen (gel) state. The formula for the dry Na Eucatex sample given in the "Experimental" section can be abbreviated as:

$$\text{Layer}^{1.3-}1.3\text{Na}^{+}$$

where the unit cell weight of 807 is composed of 777 from the vermiculite layer and 30 from the 1.3 charge balancing interlayer Na cations. The dry n-butylammonium Eucatex therefore has the formula:

$$\text{Layer}^{1.3-}1.3\text{C}_4\text{H}_9\text{NH}_3^{+}$$

and the contribution of 96 from the 1.3 n-butylammonium ions increases the unit cell weight to 873. The dry n-butylammonium Eucatex has a d-value of 1.49 nm and the wet n-butylammonium Eucatex used in the swelling experiments has a d-value of 1.94 nm (Humes 1985). Although the in-plane dimensions of the unit cell are slightly dependent on the type of isomorphous substitutions in the lattice, and the exact dimensions of the Eucatex cell are unknown, it seems reasonable to take the standard value of 0.515×0.89 nm^2 for the surface area of the cell (van Olphen 1977). This determines the number of water molecules in the wet crystalline state via the density: the volume of the unit cell is 0.89 nm^3, and this must contain 996 a.u. in order to reproduce the observed density $\rho = 1.86$ gcm^{-3}. The water therefore contributes 123 a.u. per unit cell and the formula for the wet n-butylammonium Eucatex is:

$$\text{Layer}^{1.3-}1.3\{\text{C}_4\text{H}_9\text{NH}_3\cdot 5.3(\text{H}_2\text{O})\}$$

The value of 5.3 water molecules per cation is a typical one for a hydrated crystalline vermiculite (Skipper et al. 1994).

The calculation of the surface area is now straightforward. Each cell has a surface area of 0.515×0.89 nm^2 on each side, and 996 g of the clay contains 6.02×10^{23} cells (Avogadro's number). Thus, the total surface area of 1 g of n-butylammonium vermiculite is:

$$\left(\frac{1}{996}\right) \times 6.02 \times 10^{23} \times 0.515 \times 0.89 \times 2 \text{ nm}^2 \text{ g}^{-1} = 554 \text{ m}^2 \text{ g}^{-1} \quad [5]$$

which corresponds to 1030 m^2 cm^{-3}. It is unlikely that the third figure in this number is truly significant, so we take the surface area of 1 cm^3 of the vermiculite to be 1000 m^2.

The calculation of the area occupied by 1 cm^3 of adsorbed polymer is less clear-cut. The true segment density profile of a polymer in contact with a clay surface has not, to our knowledge, been measured, but is supposed to consist of trains, loops and tails (Fleer et al. 1993). We can gain a qualitative insight by using the radius of the gyration of the polymer molecule in solution to estimate an effective volume per molecule V_{eff} as:

$$V_{\text{eff}} = \frac{4}{3}\pi R_g^3 \quad [6]$$

If we now assume that:

$$V_{\text{eff}} = A_p l_p \quad [7]$$

where A_p is the effective surface area occupied by a polymer molecule confined within a distance l_p of the surface, we can calculate the coverage if we know the effective thickness of the adsorbed layer l_p. As a first guess, we take $l_p = 1$ nm. For the most extensively studied system, the PVME-18,000 system, inserting $R_g = 5$ nm and $l_p = 1$ nm into these crude equations gives $A_p = 500$ nm^2, where only 1 significant figure has been kept because the calculation is an order of magnitude one only. As the density of the PVME is approximately 1 gcm^{-3}, 1 cm^3 of a species with $M_n = 18{,}000$ contains approximately 3×10^{19} molecules, which would occupy 1.5×10^{22} nm$^2 \approx 10{,}000$ m^2 of surface area. This is about 10 times the surface area offered by 1 cm^3 of the vermiculite. As r was held constant at 0.01, this implies that $v = 0.001$ is sufficient for complete coverage of the surface if the polymer is strongly adsorbed.

Such strong polymer adsorption would lead to displacement of n-butylammonium counterions, as well as water molecules, from the vermiculite surfaces. Displacement of the n-butylammonium counterions from the surface would lead to an increase in Z_{eff}, the effective surface charge that mediates the electrostatic interaction between the layers (Low 1987). This in turn would cause a decrease in the d-value (Sogami et al. 1991; Sogami et al. 1992). If we use Figure 7 of the exact mean field theory solution to the 1-dimensional colloid problem (Sogami et al. 1992) to estimate the change in Z_{eff} necessary to bring about a change in d from 12 to 8 nm, it corresponds to a 2 to 3 times increase. This is not impossible, because the effect of uniaxial stress on the pure aqueous gels (Crawford et

al. 1991) has shown that, at $c = 0.1\ M$, $(Z_{eff}/Z_{tot}) = 0.2$, corresponding to 80% adsorption of the *n*-butylammonium ions. An increase in the effective surface charge of ×2.5 would imply $(Z_{eff}/Z_{tot}) = 0.5$, namely that 50% of the ions were adsorbed, rather than 80% in the pure aqueous system. There are 3 problems with this mechanism, however, as discussed below.

For a compressed polymer (contained within 1 nm of the surface) occupying the same effective volume as a free chain in solution, the surface would be completely covered at all the volume fractions studied if we assume an H-type (high affinity) isotherm (Theng 1979) for the adsorption process, corresponding to (A) ≫ (C). However, such strong confinement of the polymer close to the surface in the gel phase may represent an underestimate of l_p if there are substantial numbers of segments in trains and loops. We can obtain an upper estimate for the polymer adsorption from the data collected by Theng (1979) for the plateau value of poly(vinyl alcohol) (M_n = 70,000) adsorption on clay surfaces. This was found to be remarkably similar for many 2:1 type layer silicates, ranging from 1.1 to 1.3 mg m^{-2}. This corresponds to about 1 cm^3 of polymer adsorbed onto 1 cm^3 of vermiculite in our case, or complete coverage at $v = 0.01$ for H-type adsorption. In these circumstances, the confinement distance would be given by l_p = 10 nm (approximately the same as the interlayer spacing), or $2R_g$, so the latter model is a physically reasonable one.

Our order of magnitude calculations tell us that the vermiculite can adsorb between 0.1 to 1.0 times its own volume onto surface sites, depending on the degree of flattening of the polymer configuration. Of course, in the latter model, there would also be type (D) adsorption at $c = 0.1\ M$. The approximate matching of $2R_g$ and l_p in the case when the contraction was observed suggests that type (D) adsorption might be important, namely that a substantial number of polymer molecules are physically adsorbed onto both of 2 neighboring vermiculite layers, bridging them. Such "bonds" between the vermiculite layers might have the effect of binding them more strongly and so explain results (1)–(3). However, all possible mechanisms run into the problem that they also have to explain results (4) and (5), the insensitivity of T_c and the *d*-value in the tactoids to polymer addition.

Insensitivity of T_c and the *d*-value in the Tactoids

The most remarkable feature of all our results was (4), the insensitivity of T_c to the addition of neutral polymers, and its sister result (5), that the *c*-axis *d*-value of 1.94 nm in the collapsed regions in samples with added polymer is equal to that in the pure aqueous system. Since the vermiculite layers themselves have a thickness of approximately 1 nm, the interlayer spacing in the crystalline regions is also approximately equal to 1 nm, so it is not possible for a polymer with a radius of gyration of several nanometers to exist as *free chains* inside the tactoids. Although it is possible for the polymer to be adsorbed into the 1-nm gap between the clay plates in a flattened configuration, it is unlikely that substantial polymer adsorption into the tactoids would lead to an identical interlayer spacing to that obtained in the pure aqueous system, so result (5) suggests that only a very small number of polymer molecules can be included in the crystalline regions. Whether or not this in turn suggests that there is little adsorption in the gel phase is then a question of kinetics. As the dynamics of polymer desorption are normally considered to be slow (Theng 1979) and the dynamics of the *n*-butylammonium vermiculite phase transition have been reported to be surprisingly rapid, of the order of 10 min (Smalley et al. 1989), it seems unlikely that the polymer could desorb during the time it takes for the plates to collapse. Result (5) therefore throws some doubt on the importance of sites (A) and (D).

CONCLUSION

Whatever the mechanisms, the facts are interesting in their own right. It seems unlikely that any theory could have predicted results (1)–(5) in advance of the experiments and they are all clear-cut results on a well-defined 4-component system. The general picture that emerges is that the effect of adding neutral polymers to the *n*-butylammonium vermiculite system is a surprisingly weak one, especially with regard to the insensitivity of T_c. This result is difficult to reconcile with substantial polymer adsorption onto the vermiculite surfaces and indicates that the driving force for the gel–tactoid phase transition must be strong. The electrical origin of this phase transition (Smalley 1990, 1994a, 1994b) is strongly supported by the fact that the gel phase is completely suppressed by the addition of a charged polymer.

ACKNOWLEDGMENTS

We would like to thank the Central Research Laboratories of the Kuraray Co. for the chemical analysis of the sodium and *n*-butylammonium vermiculite samples, H. Hasegawa of Kyoto University for providing us with the PVME-18,000 sample and K.A. Smalley for her assistance in the preparation of the neutron scattering samples.

REFERENCES

Braganza LF, Crawford RJ, Smalley MV, Thomas RK. 1990. Swelling of *n*-butylammonium vermiculite in water. Clays Clay Miner 38:90–96.

Brandrup J, Immergut EH. 1989. Polymer handbook. New York: J. Wiley. 65 p.

Crawford RJ, Smalley MV, Thomas RK. 1991. The effect of uniaxial stress on the swelling of *n*-butylammonium vermiculite. Adv Colloid Interface Sci 34:537–560.

Fleer GJ, Cohen Stuart MA, Scheutjens JMHM, Cosgrove T, Vincent B. 1993. Polymers at interfaces. London: Chapman & Hall. 502 p.

Garrett WG, Walker GF. 1962. Swelling of some vermiculite–organic complexes in water. Clays Clay Miner 9:557–567.

Humes RP. 1985. Interparticle forces in clay minerals [D. Phil. thesis]. Oxford, UK: Oxford Univ. p 140–153.

Jinnai H, Smalley MV, Hashimoto T, Koizumi S. 1996. Neutron scattering study of vermiculite–poly(vinyl methyl ether) mixtures. Langmuir 12:1199–1203.

Kleijn WB, Oster JD. 1982. A model of clay swelling and tactoid formation. Clays Clay Miner 30:383–390.

Lagaly G. 1981. Characterization of clays by organic compounds. Clay Miner 16:1–21.

Low PF. 1987. Structural component of the swelling pressure of clays. Langmuir 3:18–25.

Norrish K, Rausell–Colom JA. 1963. Low-angle X-ray diffraction studies of the swelling of montmorillonite and vermiculite. Clays Clay Miner 10:123–149.

Rausel–Colom JA. 1964. Small-angle X-ray diffraction study of the swelling of butylammonium vermiculite. Trans Faraday Soc 60:190–201.

Rausell–Colom JA, Saez-Aunon J, Pons CH. 1989. Vermiculite gelation: Structural and textural evolution. Clay Miner 24:459–478.

Shibayama M, Hashimoto T. 1986. Small-angle X-ray scattering analyses of lamellar microdomains based on a model of one-dimensional paracrystal with uniaxial orientation. Macromolecules 19:740–749.

Skipper NT, Soper AK, Smalley MV. 1994. Neutron diffraction study of calcium vermiculite: Hydration of calcium ions in a confined environment. J Phys Chem 98:942–945.

Smalley MV. 1990. Electrostatic interaction in macroionic solutions and gels. Mol Phys 71:1251–1267.

Smalley MV. 1994a. Electrical theory of clay swelling. Langmuir 10:2884–2891.

Smalley MV. 1994b. One phase and two phase regions of colloid stability. Progr Colloid Polym Sci 97:59–64.

Smalley MV, Thomas RK, Braganza LF, Matsuo T. 1989. Effect of hydrostatic pressure on the swelling of *n*-butylammonium vermiculite. Clays Clay Miner 37:474–478.

Sogami IS, Shinohara T, Smalley MV. 1991. Effective interaction of highly charged plates in an electrolyte. Mol Phys 74:599–612.

Sogami IS, Shinohara T, Smalley MV. 1992. Adiabatic pair potential of highly charged plates in an electrolyte. Mol Phys 76:1–19.

Tanaka H. 1993. Dynamic interplay between phase separation and wetting in a binary mixture confined in a one-dimensional capillary. Phys Rev Lett 70:53–56.

Theng BKG. 1979. Formation and properties of clay–polymer complexes. Dev Soil Sci 9:37–94.

van Olphen H. 1977. An introduction to clay colloid chemistry. New York: J. Wiley. p 254–255.

Walker GF. 1960. Macroscopic swelling of vermiculite crystals in water. Nature 187:312–313.

Williams GD, Moody KR, Smalley MV, King SM. 1994. The sol concentration effect in *n*-butylammonium vermiculite swelling. Clays Clay Miner 42:614–627.

(Received 22 July 1996; accepted 27 January 1997; Ms. 2797)